J Mol Model (2012) 18:3927–3939
DOI 10.1007/s00894-011-1297-8

ORIGINAL PAPER

Insights from comprehensive multiple receptor docking to HDAC8

Michael Brunsteiner · Pavel A. Petukhov

Received: 18 March 2011 / Accepted: 2 November 2011 / Published online: 20 March 2012

Abstract A systematic investigation of the available crystal structures of HDAC8 and of the influence of different receptor structures and docking protocols is presented. The study shows that the open conformation of HDAC8 may be preferred by ligands with flexible surface binding groups, as such a conformation allows the ligands to minimize their exposure to solvent upon binding. This observation allowed us to rationalize the excellent potency of pyrazole-based inhibitors compared to that of isoxazole-based inhibitors.

Keywords Histone deacetylase 8 · Docking · Multiple receptor · Binding site flexibility

Introduction

Histone deacetylases (HDAC) comprise a group of proteins that were first described in the context of histone deacetylation as part of the machinery for the control of gene transcription [1]; since then, they have been found to have various other regulatory functions [2]. The interest in HDACs and their inhibitors from the perspectives of basic biology and therapeutic applications is hard to underestimate. Most notably, they are considered a promising cancer target [3], with two HDAC inhibitors—suberoyl anilide hydroxamic acid (SAHA, vorinostat, **1a**, Table 1) and romidepsin—currently being used in the treatment of cutaneous T-cell lymphoma, and a number of other compounds in various phases of clinical development. In humans, at least 11 classical isoforms (HDAC1–HDAC11) are expressed, which are grouped into three classes (classes I, II, and IV), and each of the 11 isoforms appears to have a distinctive function and possibly different therapeutic potentials [4]. For this reason, isoform-selective HDAC inhibitors are of particular interest, but very few drug-like compounds with clear selectivity profiles have been proposed to date [4, 5].

Molecular modeling and simulation have been used as tools in research aimed at finding HDAC inhibitors with improved activity and/or selectivity. This work has included the generation of various types of QSAR models [6–11], or the docking of inhibitors to protein models followed by a discussion of docking poses [9, 12–18]. These studies provide interesting insights into structure–activity relationships, and, in at least one case, impressive accuracy in the prediction of ligand activities for an external test set [11]. However, few of these structure-based studies have concentrated on the HDAC8 isoform and the flexibility of its binding site [19–21]. The modeling of HDAC8 and its inhibitors appears to be a challenging task due to a number of issues, as outlined below.

Interactions between inhibitors and the catalytic zinc ion found in HDAC binding sites are difficult to model accurately. A recent study showed that "out of the box" docking to metalloenzymes, including those containing Zn ions, can be

Electronic supplementary material The online version of this article (doi:10.1007/s00894-011-1297-8) contains supplementary material, which is available to authorized users.

M. Brunsteiner · P. A. Petukhov (✉)
Department of Medicinal Chemistry and Pharmacognosy,
College of Pharmacy, University of Illinois at Chicago,
833 South Wood Street,
Chicago, IL 60612, USA
e-mail: pap4@uic.edu

Present Address:
M. Brunsteiner
Institute of Biotechnology and Biochemical Engineering,
Graz University of Technology,
Petersgasse 12/1,
8010 Graz, Austria

Table 1 HDAC8 inhibitors used in this study

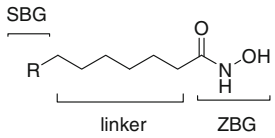

Comp. No.	Ki[μM]	R (SBG)
1a	0.395	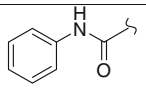
1b	6.594	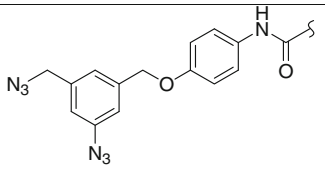
1c	0.616	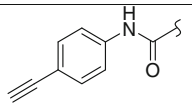
1d	0.453	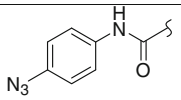
1e	2.431	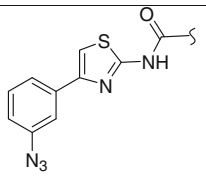
2a	0.015	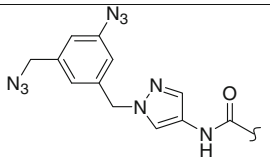
2b	0.068	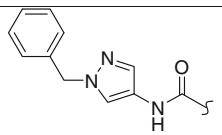

successful when applied in virtual screening campaigns, but its accuracy is limited and a rigorous parameterization of the metals is likely to be required for lead optimization [22, 23]. As opposed to most other metal ions commonly found in proteins, zinc can have three different coordination numbers. An accurate description of the Zn–ligand interactions and an evaluation of their contribution to the binding energy can probably not be achieved without resorting to high-level ab initio calculations. Attempts have been made to generate more accurate classical model potentials for zinc by including bonded energy terms between the zinc and the atoms chelating with it [24, 25]. However, such potentials require a priori knowledge of the coordination number, the calculation of protein–ligand interaction energies when the two are connected by bonds is not a straightforward task, and to our knowledge no thorough evaluation of their ability to improve the accuracy of calculated protein–ligand interaction energies is available.

The part of a typical HDAC ligand [3] that binds to the Zn^{2+} ion at the bottom of the active site of HDAC—the zinc-binding group (ZBG)—is connected to a more hydrophobic linker that extends through a tunnel towards the binding site entrance, towards the so-called surface-binding or CAP group (SBG), which is partially exposed to

Table 1 (continued)

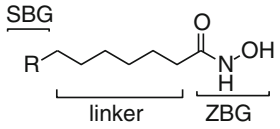

Comp. No.	Ki[μM]	R (SBG)
2c	0.074	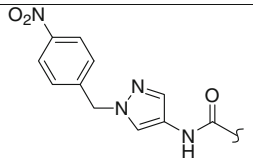
2d	0.025	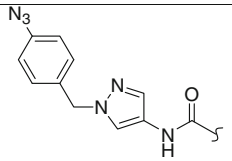
3a	0.585	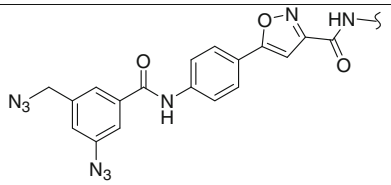
3b	0.635	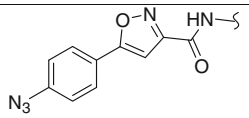
4a	0.209	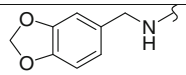
4b	0.095	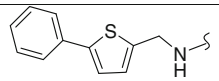

the solvent. It has been argued that variations of the SBG can potentially lead to isoform-selective inhibitors [26], as the residues residing at the binding site entrance show variations in different isoforms. In many cases, the SBG of HDAC inhibitors is relatively large, flexible, and solvent exposed. For conventional docking/scoring approaches, this makes the reliable determination of the SBG's conformation, and its contribution to the binding energy, difficult. The situation is exacerbated by the fact that some of the residues on the surface of an HDAC protein, close to the binding site, are very flexible [26], rendering traditional docking to a single rigid receptor structure unreliable. This flexibility includes extensive backbone movements due to two flexible loops. Such large variations cannot be accounted for by allowing for limited side-chain flexibility as implemented in a number of docking programs [27, 28]. One of these loops (residues Pro91–Thr105, loop A) appears to be disordered in the apoprotein [29], but it has a similar conformation in all existing crystal structures with a bound ligand [26, 29–31]. In particular, the crucial Asp101 residue, which can form a hydrogen bond with a ligand, shows some variation in terms of its orientation, but is generally in the same location throughout (Fig. 1). This is not true for the second loop (residues Ser30–Lys36, loop B), which was found in two distinctively different conformations in co-crystal structures: open (1VKG, 1T64) and closed (1T67, 1T69, 1W22, 2V5X, 2V5W) [26], resulting in the presence or absence of a second pocket next to the primary HDAC binding pocket (Fig. 1), depending on the ligand. In a recent study, Wiest et al. [21] explored the flexibility of the HDAC8 binding site using molecular dynamics simulations and confirmed that the binding site of HDAC8 is indeed rather malleable and that, if required, it can be subjected to induced-fit conformational changes to accommodate the ligands. In addition, the interpretation of the binding poses may be biased due to the fact that the

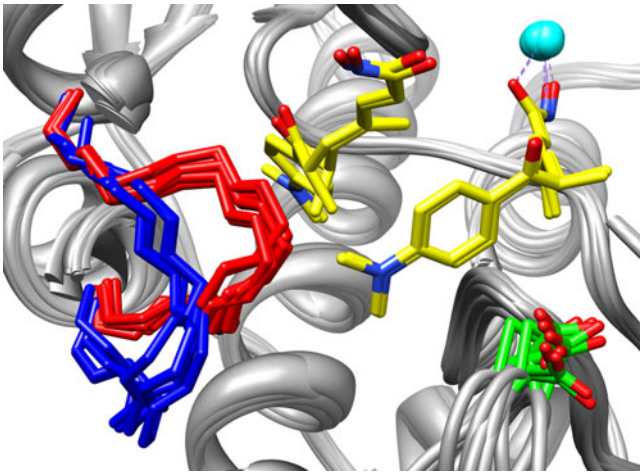

Fig. 1 Twelve aligned and superimposed HDAC8 monomers. The backbones corresponding to loop B are highlighted in *red* (closed) or *blue* (open). Also shown are the TSA ligands in PDB:1T64; one TSA occupies the primary pocket, interacting with the zinc (*cyan*); the other occupies the secondary pocket, which is available only if loop B is open. Asp101, representing the tip of loop A, is shown in *green*

conformation of the HDAC ligand that co-crystallize with HDAC8 is influenced by the interactions between the ligand and neighboring copies of the protein and/or ligand in the crystal lattice, as evidenced by analysis of the X-ray structures of HDAC8. When the protein is solvated under physiological conditions, the conformation of the SBG may differ from that seen in crystal structures, making interpretation even more complicated.

Clearly, the problem of modeling the binding poses of HDAC inhibitors remains one of the key challenges in HDAC inhibitor structure-based drug design. To address it, we recently developed a binding ensemble profiling with photoaffinity labeling (BEProFL) approach that utilizes a diazide probe to experimentally map the multiple binding poses of the SBGs of HDAC ligands [32]. We also designed and synthesized several highly potent cell-permeable HDAC isoxazole- and pyrazole-based photoreactive probes [33]. Interestingly, we found that our probe **1b** (Table 1) was able to crosslink to the residues at the bottom of the second pocket in the open conformation of HDAC8 PDB:1T64 mentioned above. We also found that, despite the presence of relatively bulky and lipophilic diazide moieties (necessary for BEProFL) in the SBGs, both the isoxazole- and the pyrazole-based probes exhibited excellent low double-digit nanomolar inhibitory activities against HDAC3 and HDAC8. With an IC_{50} of 17 nM, the pyrazole-based probe **2a** (Table 1) is one of the most active HDAC8 inhibitors reported to date. On the basis of these data, we hypothesize that even for ligands (or photoreactive probes) that do not require substantial conformational changes, the ligands and their SBGs have the opportunity to bind to either the closed or the open conformations of the HDAC8 protein, allowing the SBGs of the ligands to minimize solvent exposure and gain additional interactions with the protein. This would be a significant departure from the published protocol for docking to HDAC8, and may open new directions in the design of inhibitors that may target the open conformation instead of or in addition to the closed conformation of HDAC8. To our knowledge, in all previous docking studies using HDAC8 binding data (with the exception of our publications [32, 33] and a study by Wiest et al. [21]), only receptors based on a crystal structure with closed loop B were used [19, 34]. In this paper, we present and rationalize a multiple receptor docking and scoring study of a series of novel HDAC8 inhibitors docking to a set of the closed and open conformations of the HDAC8 protein.

Materials and methods

Modeling

Coordinates of HDAC8 protein structures were downloaded from the Protein Data Bank (PDB) [35]. Visual inspection of the crystal structures (PDB IDs 1T64, 1T67, 1T69, 1VKG, 1W22, 2V5W, and 2V5X) [26, 29–31] was performed using Chimera [36]. Reconstruction of the full unit cell was performed, starting from each PDB file using the Python script crystalcoords.py in Chimera. The resulting coordinates, containing all copies of the asymmetric unit in the unit cell of each HDAC8 crystal structure, were analyzed with Chimera and in-house awk scripts to establish contacts between the different symmetry copies of the HDAC8 monomer. All protein copies closer than 10 Å to the ligand in the primary binding site were identified for the re-docking of the native ligands. This typically included only one extra protein chain. The resulting two HDAC monomers were then saved and used as a single protein for docking.

The five crystal structures (1T64, 1VKG, 1W22, 2V5X, 2V5W) that contained two nonequivalent protein chains in the asymmetric unit were split to yield two different receptor structures. Two structures (1T67 and 1T69) contained only one chain per asymmetric unit. Taken together, this provided twelve different receptor structures. Conserved water molecules were identified by splitting the HDAC8 crystal structures into the monomers, aligning and superposing them using the Matchmaker tool in Chimera, and then inspecting visually. All water molecules that were found in less than three out of the twelve HDAC8 monomers were discarded, resulting in only two conserved clusters of water molecules. The oxygen atoms of the two water clusters identified in this way were saved, and the center of mass of each cluster was used as the oxygen

position in all receptor structures used for docking. The receptor set was further extended by adding to each structure either zero (W0), one (W1), or both (W2) of the water molecules. The resulting 36 receptor structures are labeled accordingly (e.g., 1T64B-W2 is the label for the receptor based on chain B of the structure with PDB:1T64 plus both water molecules W1 and W2).

If present, gaps in the sequence of each monomer were filled, and the resulting coordinates were subsequently refined, using the homology modeling program Modeller [37]. Specifically, the structure 2V5X was used as a template for modeling the unresolved amino acids in monomers of HDAC8 with the missing residues. 2V5X was chosen because it has a reasonably good resolution (R=2.25 Å), and has all the residues resolved. The geometries and positions of the newly modeled residues were further refined by a Monte Carlo simulation using a built-in Modeller empirical force field. The resulting HDAC8 monomers were protonated using the program Reduce [38]. This program analyzes the hydrogen bond network in each monomer and adjusts (flips) Gln, Asn, and His side chains accordingly. The protonation states of the proteins were then fixed and the water oxygen atoms were protonated using MOE [39]. The ligands were prepared using MOE [39], and we chose deprotonated hydroxamic acid (HA) for each ligand [40]. For the re-docking experiments, the same procedure was followed using either one monomer or the entire unit cell.

The programs GOLD [41] and Surflex-dock [42] were used for docking/scoring, and default parameters and settings were used unless mentioned explicitly. The native ligand in each monomer structure was used to define the binding site. Docking was performed with zero, one, or two conserved water molecules as part of the receptor structure. The atoms of the HA group were constrained to their experimental positions using a weight of 5 (GOLD) or 10 (Surflex-dock). It was found in preliminary studies that these values for the force constants give poses with comparable HA geometries.

Some of the compounds used here contain azide groups, and preliminary studies with Surflex-dock showed that the DREIDING force field [43] employed by this program was unable to reproduce the angle of nearly 180° formed by the three azide nitrogen atoms [44]. Since Surflex-dock does not allow the force field parameters used to be edited, we decided to replace the azide N=N=N by a sufficiently similar moiety for the docking calculations. As, in each case, the magnitude of the AM1BCC partial charge [45] calculated with Molcharge [46] was lower than 0.3 for the two terminal nitrogen atoms of the azides, we concluded that this residue is best modeled as a hydrophobic moiety. Given this, the approximate nature of a scoring function, and the similar van der Waals radii of the two residues, we concluded that an N=C=CH_2 group—which does give the correct linear geometry [44]—can be used as an analog mimicking the azido group.

When docking with Surflex-dock, the *pgeomx* flag was used to ensure a more exhaustive search; this resulted in GOLD and Surflex-dock using approximately the same amount of CPU time per compound. Twenty poses were generated for each ligand/receptor combination.

All ligands docked with Surflex-dock were processed by deleting the HA group and four of the six CH_2 units of the linker connecting ZBG and SBG. This task was automated using in-house awk scripts and programs based on the openbabel C library, version 2.2 [47]. The same settings were used when re-scoring the resulting fragments with the HA group removed as in the original docking runs. This protocol is referred to as SC2, and the protocol for scoring the entire ligand as SC6. Additional calculations were performed using fragments including zero (SC0) or four (SC4) CH_2 units.

Multiple receptor docking was done by docking to each possible pair of receptor structures and using the better of the two scores for each compound for the final ranking. The same docking procedure was used for the full ligands and the fragments. In addition, the scores calculated for the ligands and ligand fragments with each receptor structure were normalized. To do this, a histogram was generated from all of the calculated scores from each receptor structure, a normal distribution curve was fitted to each histogram using the statistical package R [48], and all individual scores were normalized by subtracting the mean and dividing by the standard deviation.

HDAC8 inhibitors and assays

The compounds considered here—**1c, 1d** (Petukhov PA et al., unpublished), **2a-d, 3a,b** [33], **1b**,**e** [32], **4a**,**b** (Petukhov PA et al., unpublished)—represent several series of new HDAC inhibitors and probes (Table 1) that were synthesized by us as a part of our project to develop photoreactive probes for BEProFL [32, 33].

The inhibition of HDAC8 was measured as recommended by the supplier BIOMOL International (Plymouth Meeting, PA, USA), using the fluorescent acetylated HDAC substrate Fluor de Lys (BIOMOL, KI178) and commercially available recombinant human HDAC8 (BIOMOL). The activity data are summarized in Table 1. The procedure is identical to that published previously [32].

Results and discussion

Analysis of co-crystal structures

An analysis of the HDAC8 crystal structures was performed to identify a set of proteins and water molecules that

were appropriate for the docking. A total of twelve wild-type HDAC8 structures co-crystallized with a hydroxamic acid based inhibitor were available at the time this study was performed. Visual inspection of the aligned monomers of HDAC8 with resolved water molecules (Fig. 2c) revealed the presence of one water molecule (W1) that forms a hydrogen bond with His180 and an acceptor atom, typically a carboxamide oxygen atom, in the ligand. This interaction pattern was found in nine of the eleven monomers. Another water molecule (W2) forms H-bonds with W1, Phe208, and, in four cases, also with a bound ligand. The RMSD of the water oxygen atoms in the W1 cluster is 0.49 Å, and this value is 0.37 Å for W2. Since including conserved water molecules may improve the accuracy of the docking [49], both W1 and W2 were considered during docking.

To further investigate the influence of crystal packing and ligand structure on the poses of SBGs and conformation of the protein, the coordinates of the full unit cell were regenerated from each of the PDB files, and interactions between the ligands and the protein residues in its vicinity were analyzed by visual inspection. In all cases, it was found that the ligand SBG interacts not only with the HDAC8 monomer it is bound to but also residues and/or ligands of neighboring copies of the protein in the crystal lattice (Fig. 2a). It is unclear whether the pose and the resulting protein–ligand interactions of a given compound's SBG would also occur under physiological conditions (i.e., in solution) or whether this pose is, at least in part, determined by interactions between the SBG and symmetry copies of the primary protein.

The generation and visual inspection of the full unit cells of HDAC8 crystal structures also highlighted another phenomenon that can possibly complicate the interpretation of co-crystal structures in the context of drug design: in nearly all cases, the smallest distance between protein residues in loop B and any atom found in one of the symmetry copies of the protein in the crystal lattice is well below 4 Å. In all structures that have a closed loop B (Fig. 1), at least one hydrogen bond is formed between loop B and an atom in another HDAC8 monomer (see Table S1 in the Electronic supplementary material). Interestingly the only structure in which no atom in loop B is in contact with other proteins in the crystal lattice is 1T64, which is one of the two structures with an open loop B. The two chains, A and B, in the asymmetric unit of 1T64 (loop B open) were aligned on the corresponding chains in the full unit cell of 1T69 (loop B closed) and are shown in Fig. 2b. We find that the two copies of loop B of the 1T64 chains overlap, with the closest distance between two non-H atoms being 1.2 Å, while this distance is 6.6 Å for the PDB:1T69 structure. The data indicate that the open and closed conformations observed in the X-ray structures may be a combined result of the conformational changes caused by a specific bound ligand and interactions between the symmetry copies. Thus, neither of the conformations can be excluded or prioritized only on the basis of the structure of the ligands.

Re-docking of native ligands

The analysis of the crystal structures of HDAC8 provided above shows that the second copy of the HDAC8 protein may affect the conformation of the HDAC8 protein and the bound ligands, and therefore we decided to determine how this would affect the results of the re-docking experiments.

HDAC inhibitors were re-docked to their native receptors, comparing the docking accuracies achieved with the two different docking protocols/scoring functions. All the co-crystal structures of hydroxamic acid based HDAC inhibitors that were available at the time of writing this paper were used for this purpose. If more than one chain was present in the asymmetric unit, the one with the lower average B factor was used. Given the results of the previous section, and to account for the effect of interactions

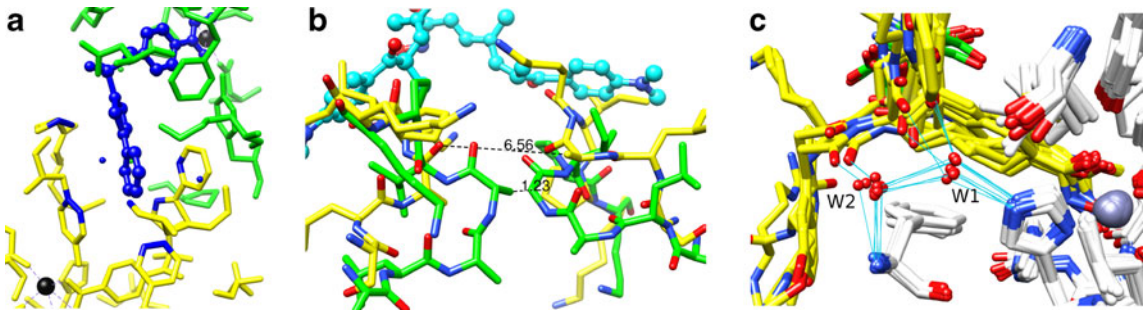

Fig. 2 Interactions between an HDAC8 protein/ligand and symmetry copies in co-crystal structures, and visualization of conserved water molecules. **a** Example of interactions between a ligand SBG (*blue*) bound to one monomer (*green*) and a symmetry copy in the crystal lattice (*yellow*). **b** Section of the unit cell of PDB:1T64 (*green*) aligned on PDB:1T69 (*yellow*). The segments of the sequences shown represent the tip of loop B, which is open in 1T64 and closed in 1T69. The closest distance between any two atoms in the two symmetry copies of the monomer are indicated for both structures. **c** Aligned HDAC8 co-crystal structures (ligands in *yellow*, protein in *white*) revealing the presence of two conserved water molecules (*red spheres*)

between the ligand SBG and symmetry copies of the HDAC8 monomers, as well as the water molecules W1 and W2 found in the majority of cases, receptor structures were set up in six different ways: (i) one HDAC8 monomer (chain A); (ii) as (i) plus W1 (chain A + W1); (iii) as (i) plus W1 and W2 (chain A + W1 + W2); (iv) one HDAC monomer plus all symmetry copies of the protein and bound ligand that can possibly come into contact with the docked ligand SBG (x-tal); (v) as (iv) plus the conserved water molecule W1 (x-tal + W1); (vi) as (iv) plus the conserved water molecules W1 and W2 (x-tal + W1 + W2). In preliminary docking runs with GOLD and Surflex-Dock, it was found that, in some cases, the best-scored docking pose corresponded to a structure with the ligand ZBG far from the protein's Zn^{2+} ion (not shown). Therefore, constraints were applied in all docking runs to ensure that the ZBG coordinates are close to their experimental values.

The results of the docking for five ligands with different protocols are shown in Table 2. Analysis of the poses obtained for 2V5X shows that the docking software tends to position the ligand such that its two indol substituents switch positions compared to those in the crystal structure. The ligand is somewhat symmetrical and can occupy almost the same space in the binding site in both the cases, making prediction of the docking poses a rather challenging task. Given the exceptionally large and flexible SBG found in 2V5X, even values of 3.70 Å and above can be considered acceptable. To minimize bias due to the unusually high RMSD values obtained for 2V5X, we excluded 2V5X from calculations of the average RMSD values given in Table 2 and the discussion below.

The RMSD values obtained with Surflex-dock are smaller if the receptor structure is constructed in the most accurate way (i.e., it includes symmetry copies of the HDAC8 protein directly adjacent to the binding site). A similar trend is observed for re-docking with GOLD, though somewhat less pronounced. Re-docking to the primary monomer structure of HDAC8 without a symmetry copy and the conserved water molecules resulted in an average RMSD that was 2.65 Å smaller for GOLD than for Surflex (Table 2). Since the SBGs of the ligands co-crystallized with HDAC8 are in the vicinity of a symmetry copy of another HDAC8, it is unclear why GOLD was able to generate poses with smaller RMSDs while Surflex was not. When re-docking to a monomer of HDAC8, the inclusion of water molecules W1 and W2 leads to a decrease in the average RMSD for Surflex of ca. 2 Å, whereas for GOLD the average RMSD increases by ca. 1 Å. In the case of "x-tal" receptors, inclusion of water molecules affects the accuracy only marginally. We note that the best RMSD values obtained for 1VKG with Surflex in particular are small, confirming that the modeled structure of loop A in 1VKG is unlikely to introduce artifacts.

In one case (1VKG), Surflex docking clearly gives a better result than GOLD docking, but in all other cases, the two docking programs and scoring functions used here show similarly good performances in terms of reproducing experimental poses in their native "x-tal," "x-tal+W1," and "x-tal+W1+W2" receptors—the entire unit cell with all symmetry copies of the primary monomer.

Since re-docking to several open and closed HDAC8 crystal structures containing the second copy of the HDAC8 protein generally resulted in improved RMSD values, neither of the crystal structures should be excluded based on the re-docking accuracy, and we elected to use a

Table 2 Re-docking of native ligands to HDAC8 co-crystal structures. Results obtained with two docking programs/scoring functions are given as RMSD values between experimental and docked ligands. The receptor structures used for docking are: one monomer (chain A), one monomer plus one or two conserved water molecules in the binding site (chain A+W1, chainA +W1+W2), the entire unit cell with all symmetry copies of the primary monomer (x-tal), and the entire unit cell plus one or two conserved water molecules in the binding site (x-tal+W1, x-tal+W1+W2)

PDB	Surflex-dock score						GOLD score					
	Chain A	Chain A+W1	Chain A+ W1+W2	X-tal	X-tal+W1	X-tal+ W1+W2	Chain A	Chain A+W1	Chain A+ W1+W2	X-tal	X-tal+W1	X-tal+ W1+W2
1T64	1.18	1.12	1.80	0.63	2.07	2.29	1.19	0.91	0.96	0.43	0.43	0.91
1T67	5.95	1.78	2.18	1.57	1.31	1.43	2.40	2.40	2.43	2.01	0.96	0.68
1T69	4.74	4.60	4.40	1.86	1.88	4.65	1.87	1.94	1.96	1.85	1.76	1.87
1VKG	6.06	6.36	3.44	1.50	0.96	2.05	3.80	9.20	9.16	3.54	3.41	1.25
1W22	7.32	7.19	2.97	1.97	1.30	0.98	2.73	2.72	2.74	1.53	1.48	1.25
2V5X	5.52	8.66	9.63	5.93	4.41	7.72	4.54	8.88	10.82	5.09	5.06	3.70
Average RMSD[a]	5.05	4.21	2.96	1.51	1.50	2.28	2.40	3.43	3.45	1.87	1.61	1.19

[a] RMSD values for 2V5X were excluded from averaging

multiple receptor docking protocol. Inclusion of multiple receptor structures in the docking to account for large variations in protein conformation has become a commonly applied strategy [50–54]. Despite the better accuracy observed for the "x-tal"-based receptors, we could not use them for docking ligands other than native ones, so all of the following studies were performed only with the monomers of HDAC8.

Docking to single receptors

Receptor structures based on twelve different HDAC8 monomers were prepared as described in "Methods," and zero, one, or two water molecules were added to each structure, resulting in 36 receptor structures for docking. The compounds in Table 1 were docked to each of the receptor structures using two different docking programs, Surflex-dock and GOLD. Constraints on the hydroxamic acid group and other parameters were used as described in "Methods." The pK_i values for all compounds were compared to the calculated docking scores, resulting in 36 correlations (Pearson correlations) each for the GOLD (not shown) and the Surflex-dock (Fig. 3a) results. The Pearson correlations were used to differentiate between positive and negative correlation. The correlations show a clear positive trend. Both the average and the best (average r=0.17, best r =0.43) correlations obtained from the GOLD results are somewhat poorer than those obtained with Surflex-dock (average r=0.23, best r=0.67). Taking into account that Surflex-dock was also successful at re-docking native HDAC ligands, and that it contains a desolvation term, we decided to perform the calculations discussed below based only on the Surflex-dock results. In the following we employ two techniques—a variation of fragment-based scoring and multiple receptor-based docking—to evaluate their effects on the results of docking/scoring calculations.

Fragments

To avoid difficulties with the parameterization of the Zn^{2+} ion in the HDAC active site, we decided to explore how truncation of the ZBG would affect the docking. Specifically, the docking poses generated as described in the previous section were processed by removing the hydroxamic acid moiety and a part of the linker from each docked ligand, and the resulting fragments were then re-scored. Here we make the assumption that the contribution from the Zn^{2+}–ZBG interactions is similar for all ligands, and that these contributions cancel out to a good degree. The best correlation obtained from fragment-based scores (SC2) is r= 0.74 for receptor structure 1VKGB-W0. For the full ligands (SC6), the best correlation was weaker, with r=0.67 for receptor structure 2V5WB-W0. In both cases (SC2 and SC6), the best correlations were substantially higher than the average correlations of r~0.2 (Table 3). We also performed equivalent calculations for ligands that were truncated to leave fragments with four (SC4) or zero (SC0) instead of two (SC2) CH_2 units of the linker. The correlations obtained with SC0 were somewhat weaker, and those with SC4 were comparable to the correlations from the SC2 protocol. The top two receptor structures in terms of the resulting correlations were identical for SC2 and SC4 (2V5XA-W2 and 1VKGB-W0). The correlations obtained with the three protocols SC0, SC2, and SC4 for all receptor structures are similar, and show good correlations of r>0.8 between each other, while the same kind of correlation between SC6 and the three other protocols is smaller than r=0.7 in all cases.

We found that the truncated form of this type of HDAC8 inhibitor can be used instead of the full ligand, leading to a slight improvement in correlation between the docking scores and the experimental affinities. The relative scores were also not very sensitive to the precise form of truncation chosen. This is particularly important, as the ionization states of the ligands and residues [55, 56] and the identity of the metal ion in the HDAC active site [57] have been a matter of debate. In the following we only discuss the results obtained with the SC6 and SC2 protocols.

Multiple receptors

The docking scores obtained with each compound/receptor combination were chosen from all possible pairs of receptor structures using the best out of two scores for each compound. This was done independently for the results from both the SC2

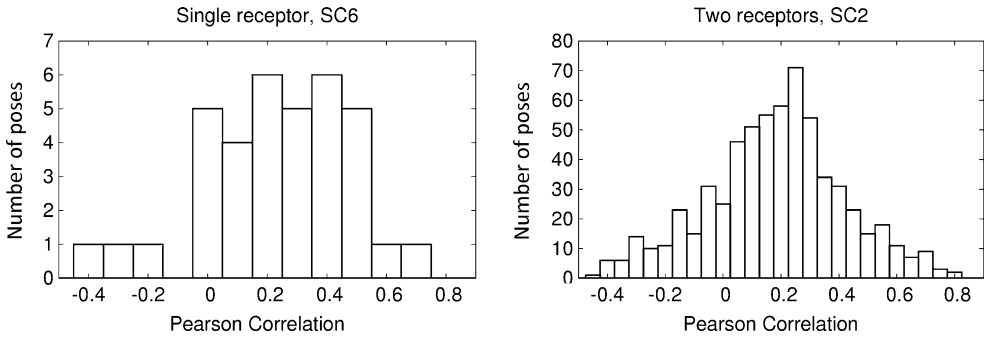

Fig. 3 **a** Histograms of the correlations between experimental affinities and scores from docking to single receptors and SC6 scoring the entire ligand. **b** The same as **a** for the multiple receptor docking protocol with a combination of all pairs of HDAC8 receptors and the SC2 scoring protocol

Table 3 Average and best Pearson correlations between experimental and calculated activities obtained using the SC2 and SC6 docking scores from single receptors (top), multiple receptors (center), or the normalized scores from multiple receptors (bottom). Also included is/are the receptor structure(s) giving the best correlation

Protocol	Avg.	Best	Recpt. 1	Recpt. 2
Single receptor				
SC6	0.23	0.67	2V5WB-W0	-
SC2	0.21	0.74	1VKGB-W0	-
Two receptors				
SC6	0.22	0.67	1VKGB-W0	2V5WB-W0
SC2	0.20	0.78	1VKGB-W0	2V5XA-W1
Two receptors, normalized scores				
SC6	0.20	0.72	2V5WB-W0	1T69A-W2
SC2	0.18	0.80	1VKGB-W0	2V5XA-W2

and SC6 protocols using the normalized scores. A summary of the results is given in Fig. 3b and Table 3. The best correlations achieved with two receptors were 0.72 for SC6 and 0.80 for SC2. With SC6, two out of 630 combinations give correlations of better than r=0.70. For SC2, this applies to 11 out of 630 combinations. On average, the resulting 630 new correlations for each of the two scoring protocols considered did not improve substantially. However, in the majority of cases, the correlations are above zero, and—compared to the single receptor SC6 protocol—we find more cases in which the correlations are particularly good, with r> 0.7. The best correlation of r=0.80 is obtained with the SC2 protocol by combining open 1VKGB-W0 and closed 2V5XA-W2 receptor structures (Table 3 and Fig. 4).

We also compared the results obtained by choosing from all possible combinations of three receptor structures and choosing from all 36 receptors. The latter gave a correlation of close to zero (r=0.02), while the best correlation obtained with a combination of three receptors is r=0.83, only a marginal improvement over the best correlations with two receptors. Therefore, and in order to keep results more interpretable, we decided to only consider results from pairs of receptors.

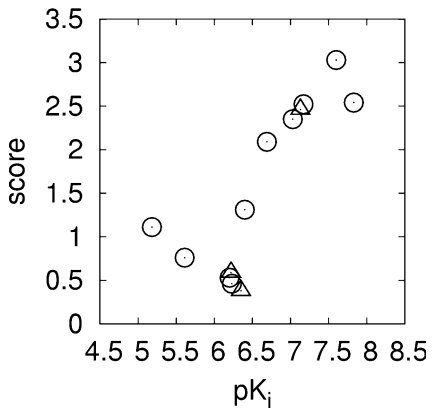

Fig. 4 Correlation between measured and predicted activities for the training set. Results were obtained from multiple receptor docking using the best out of two scores from docking to two receptor structures: 1VKGB-W0 (*open spheres*) and 2V5XA-W2 (*triangles*), with normalized fragment-based scores

Given the large number of combinations of receptors we consider here, it was important to understand the extent to which the good correlations are fortuitous. Thus, we then evaluated a test set of HDAC8 inhibitors generated by a different laboratory and performed an analysis of the trends observed with the open and closed conformations of HDAC8 for the training and test sets, as described below.

Test

Our dataset of HDAC8 inhibitors has the largest published range of HDAC8 activities among SAHA-like HDAC8 inhibitors. Although SAHA, and SAHA derivatives, belong to the most widely discussed HDAC inhibitors, the available affinity data generated using the same biological protocol in the same laboratory for the compounds based on this scaffold appear to be rather limited. We decided to use a subset of compounds published by Chen et al. [58]. The data in this paper include IC_{50} values for 17 hydroxamic acid-based HDAC8 inhibitors with flexible linkers, as used in the training set. Since the activities of these compounds only cover one order of magnitude, we decided to only use a subset of six compounds—those with the three lowest and those with the three highest IC_{50} values, resulting in two groups of compounds that are separated by about one log unit in their activities. The docking scores were then analyzed using a confusion matrix of true and false positives (TP, FP) and true and false negatives (TN, FN), respectively. The ability of the scores to categorize the ligands into weaker or stronger binders was calculated as the accuracy a=(TP+TN)/(TP+TN+FP+FN). A value of a=0.5 implies-random categorization, and a value of a=1.0 implies perfect categorization. Using the protocol that gave the best results for our training set (i.e., the best of two fragment-based scores for the receptor structures 1VKGB-W0 and 2V5XA-W2), we obtain an accuracy of a=0.67. A clearer and statistically more significant picture emerges if one considers the entire range of results obtained with all possible receptor combinations. Of all the calculated accuracies, 93% lie above and only 7% at or below a=0.5. If the docking protocol used here was unable to correctly categorize compounds with weaker or stronger activities, these numbers would reside around 50%.

Trends

To reduce the number of cases taken into account when using pairs of receptors, and to determine the difference in the trends observed with open and closed structures of

HDAC8, we split the 630 combinations of structures into three groups: one containing only pairs of structures with an open loop B (O-O), one with a combination of one open and one closed structure (O-C), and a third with pairs of two closed structures (C-C). The data were analyzed by calculating, for each group, the percentage of the receptor pairs that give a correlation above a certain threshold for the compounds in the training set. When the threshold is −1, this percentage is simply the total amount of receptor combinations in each group divided by the number of all combinations: about 10, 44, and 46% for O-O, C-C, and O-C, respectively. If the threshold is raised, the sum of the three percentages is still 100%, but the three numbers reflect the relative propensity of each group to give increasingly good correlations. As the threshold increases further (Fig. 5), there is a clear trend towards better correlations for the O-C and O-O cases, whereas the C-C combinations of receptor structures fall behind, and at correlations with $r \geq 0.7$, 100% of all cases are from either the O-C or the O-O groups.

A similar analysis was performed with the test set compounds. Figure 6 shows the accuracies achieved with all possible combinations of receptor structures for the test set in a 2D diagram. Each point represents a particular combination of receptors, and is colored according to the resulting accuracy: from zero (white) to one (black). In this diagram, the four left columns and the four bottom rows represent open structures, while the remaining columns and rows represent closed structures. The diagram clearly demonstrates a trend for the open structures 1VKG and 1T64 alone and in combination with the closed structures 1T67, 1T69, 1W22, 2V5X, and 2V5W to provide better accuracies than combinations of the closed structures 1T67, 1T69, 1W22, 2V5X, and 2V5W alone. The average

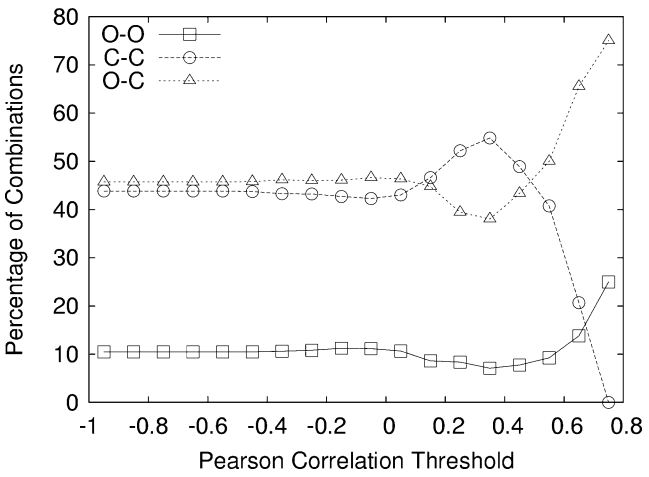

Fig. 5 The percentage of all correlations between the measured and predicted activities for the training set that are above a threshold (given on the *x*-axis), as obtained with a combination of two open (O-O), two closed (C-C), or one open and one closed (O-C) receptor structures

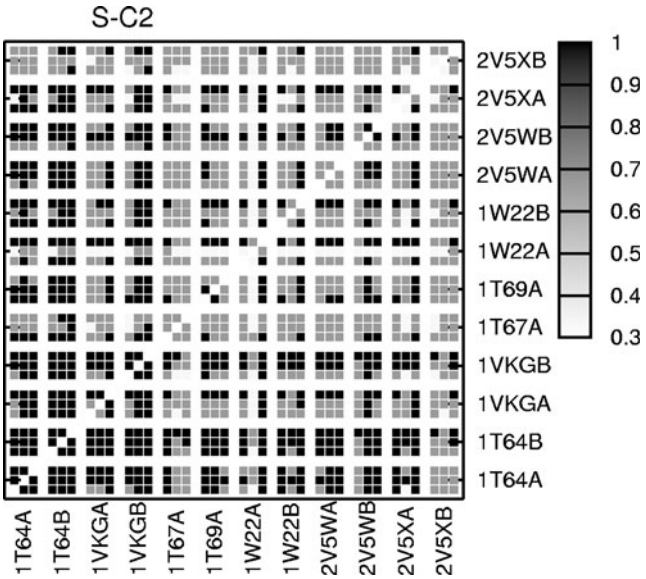

Fig. 6 Accuracies obtained for the test set compounds with all combinations of two receptor structures used in multiple receptor scoring. Each *row* and *column* is labeled according to the PDB code of the crystal structure the receptor was based upon. In each single column and row, three entries represent the different water occupancies W0, W2, and W2 in this order from *left to right* and from *top to bottom*

accuracy obtained with O-O combinations is 0.96; for O-C it is 0.83; and for C-C it is 0.71.

The receptor combination 1VKGB-W0 and 2V5XA-W2 that was found to give the best correlation for the training set also gives an accuracy of above $a=0.5$ for the test set, but there are other combinations of receptors that give better results for the test set. We believe that the reason for this is that the test set only contains compounds with large and flexible SBGs, while the training set includes a number of smaller compounds, such as SAHA. Interestingly, we see that if we perform multiple receptor scoring for the test set compounds with combinations of two different open receptors only (Fig. 6), then 60 out the possible 66 combinations give an accuracy of $a=1.0$, meaning that all six compounds are correctly assigned to one of the groups with weaker or stronger activities.

More interesting than the correlations from particular docking results is the general trend we observe for correlations. They are noticeably better if receptors based on HDAC8 structures with an open loop B are included in a set of multiple receptors. This may suggest that the SBGs of at least some of the ligands may not necessarily be solvent exposed but may instead be hidden in the open conformations of the HDAC8 protein. Moreover, the availability of both the closed and the open conformations would be consistent with the photolabeling results obtained by us with probe **1b**, which was found to photocrosslink to the residues on the surface and the residues at the bottom of the

second binding site [32]. The possibility of a dynamic equilibrium between the open, closed, and other conformations of the protein was recently highlighted by Wiest et al. [21].

These results suggest that, depending on the geometry and the size of the SBG, the ligands may preferentially bind to an open structure, which gives them an opportunity to bury their possibly bulky and largely hydrophobic SBG, or to a closed conformation of the protein if their SBG is small or cannot be accommodated by the open conformation. Indeed, we find that, with the best protocol used here, inhibitors **1c** and **1d** (two of the three compounds with the smallest SBGs) do give a better score when docked to the closed 2V5XA-W2 conformation rather than the open 1VKGB-W0 conformation. Also, nine out of the ten larger compounds give a better score when docked to the open structure. The best scoring poses of compounds **2a**, **2b**, **2d**, and **4b** (four out of the five compounds with pK_i values above 7) have their SBGs buried in the second binding pocket. This would also be consistent with the SAR we recently presented for the pyrazole- and isoxazole-based photoreactive ligands/probes [33] **2a**–**d** and **3a**, **b**, respectively. The SBGs of neither **3a** nor **3b** are small or flexible enough to fit in the second pocket, so they occupy one of the shallow grooves on the protein surface. Unlike the rigid SBG of the isoxazole-based ligands in series **3**, the SBG of the pyrazole-based ligands is smaller and more flexible. Accordingly, the majority of the pyrazole-based ligands bind to the open conformation of HDAC8 (Fig. 7, only **2a** is shown for clarity), where they have an opportunity to hide their SBG in the second binding site.

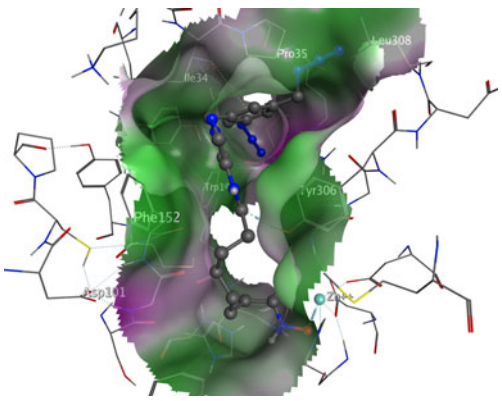

Fig. 7 Ligand **2a** docked to the binding site of HDAC8 (PDB: 1VKG, chain **B**). The space available to the ligands is the rendered surface, which is colored according to lipophilicity: *green* is lipophilic, *purple* is hydrophilic

Summary

The availability of the second binding site in the open conformation of HDAC8 for binding SAHA-like ligands was explored using multiple receptor fragment based docking. Analysis of the crystallographic structures of the HDAC8 protein indicated that the second copy of the HDAC8 protein present in the crystal lattice may affect the conformations of both of the residues in the binding site and the vicinity and the binding pose of the ligand, making it important to include the second copy of the HDAC8 protein during re-docking. Re-docking the native ligands confirmed that both Surflex and GOLD performed comparably well. The RMSD values for poses generated by both Surflex and GOLD were found to be particularly small when a monomer of HDAC8 was used in combination with the symmetry copy of HDAC8. Inclusion of the conserved water molecules during re-docking affected the accuracy of the docking for some of the X-ray structures, but not the others. The average RMSD obtained when re-docking the native ligands to the HDAC8 monomers without the corresponding symmetry copies was somewhat smaller for GOLD than for Surflex.

Neither of the open or closed conformations of the HDAC8 protein was found to be superior, and they produced comparable RMSDs in the re-docking experiments, indicating that neither the open nor the closed conformation can be excluded from consideration. To facilitate the handling of the HDAC8–Zn^{2+}–ligand complex by the docking force field, the ligands were truncated at various positions of the flexible aliphatic linker. The fragment-based docking scores were shown to be relatively insensitive to the position of the truncation. A total of 630 receptor structures containing six open and closed structures of HDAC8 and up to two conserved water molecules were used for the docking of thirteen compounds in the training set and six compounds in the test set. We found that there is a clear trend towards better correlations between pK_i against HDAC8 and the docking scores for O-C and O-O cases. At correlations with $r \geq 0.7$, 100% of all cases are from either the O-C or the O-O groups. A similar trend is observed for test set compounds: docking to the open structures 1VKG and 1T64 alone and in combination with the closed structures 1T67, 1T69, 1W22, 2V5X, and 2V5W resulted in more accurate differentiation between weaker and stronger binders overall than docking to the closed structures 1T67, 1T69, 1W22, 2V5X, and 2V5W alone. This trend is also consistent with the SAR for a series of potent HDAC inhibitors that was recently published by us. Unlike the SBG of the isoxazole-based ligands, the SBG of the pyrazole-based ligands is flexible enough to occupy the second binding pocket found in the open conformations of HDAC8. Further exploration

of novel ligand scaffolds that can utilize the second binding site of HDAC8 is underway in our laboratory.

Acknowledgments This study was in part funded by the National Cancer Institute/National Institute of Health grant R01 CA131970 and Alzheimer's Drug Discovery Foundation grant 20101103. We also thank Ajay Jane for providing a free academic version of Surflex-dock. Molecular modeling was in part conducted using free academic licenses for the UCSF Chimera package from the Resource for Biocomputing, Visualization, and Informatics at the University of California, San Francisco (supported by NIH grant P41 RR-01081) and OpenEye Scientific Software, Santa Fe, NM, USA.

References

1. Rundlett SE, Carmen AA, Kobayashi R, Bavykin S, Turner BM, Grunstein M (1996) HDA1 and RPD3 are members of distinct yeast histone deacetylase complexes that regulate silencing and transcription. Proc Natl Acad Sci USA 93:14503–14508
2. Kouzarides T (2000) Acetylation: a regulatory modification to rival phosphorylation? EMBO J 19:1176–1179. doi:10.1093/emboj/19.6.1176
3. Villar-Garea A, Esteller M (2004) Histone deacetylase inhibitors: understanding a new wave of anticancer agents. Int J Cancer 112:171–178. doi:10.1002/ijc.20372
4. Balasubramanian S, Verner E, Buggy JJ (2009) Isoform-specific histone deacetylase inhibitors: the next step? Cancer Lett 280:211–221. doi:10.1016/j.canlet.2009.02.013
5. Khan N, Jeffers M, Kumar S, Hackett C, Boldog F, Khramtsov N, Qian X, Mills E, Berghs SC, Carey N, Finn PW, Collins LS, Tumber A, Ritchie JW, Jensen PB, Lichenstein HS, Sehested M (2008) Determination of the class and isoform selectivity of small-molecule histone deacetylase inhibitors. Biochem J 409:581–589. doi:10.1042/BJ20070779
6. Chen YD, Jiang YJ, Zhou JW, Yu QS, You QD (2008) Identification of ligand features essential for HDACs inhibitors by pharmacophore modeling. J Mol Graph Model 26:1160–1168. doi:10.1016/j.jmgm.2007.10.007
7. Guo Y, Xiao J, Guo Z, Chu F, Cheng Y, Wu S (2005) Exploration of a binding mode of indole amide analogues as potent histone deacetylase inhibitors and 3D-QSAR analyses. Bioorg Med Chem 13:5424–5434. doi:10.1016/j.bmc.2005.05.016
8. Ragno R, Simeoni S, Rotili D, Caroli A, Botta G, Brosch G, Massa S, Mai A (2008) Class II-selective histone deacetylase inhibitors. Part 2: alignment-independent GRIND 3-D QSAR, homology and docking studies. Eur J Med Chem 43:621–632. doi:10.1016/j.ejmech.2007.05.004
9. Ragno R, Simeoni S, Valente S, Massa S, Mai A (2006) 3-D QSAR studies on histone deacetylase inhibitors. A GOLPE/GRID approach on different series of compounds. J Chem Info Model 46:1420–1430. doi:10.1021/ci050556b
10. Zhu Y, Li HF, Lu S, Zheng YX, Wu Z, Tang WF, Zhou X, Lu T (2010) Investigation on the isoform selectivity of histone deacetylase inhibitors using chemical feature based pharmacophore and docking approaches. Eur J Med Chem 45:1777–1791. doi:10.1016/j.ejmech.2010.01.010
11. Tang H, Wang XS, Huang XP, Roth BL, Butler KV, Kozikowski AP, Jung M, Tropsha A (2009) Novel inhibitors of human histone deacetylase (HDAC) identified by QSAR modeling of known inhibitors, virtual screening, and experimental validation. J Chem Info Model 49:461–476. doi:10.1021/ci800366f
12. Di Micco S, Terracciano S, Bruno I, Rodriquez M, Riccio R, Taddei M, Bifulco G (2008) Molecular modeling studies toward the structural optimization of new cyclopeptide-based HDAC inhibitors modeled on the natural product FR235222. Bioorg Med Chem 16:8635–8642. doi:10.1016/j.bmc.2008.08.003
13. Grolla AA, Podesta V, Chini MG, Di Micco S, Vallario A, Genazzani AA, Canonico PL, Bifulco G, Tron GC, Sorba G, Pirali T (2009) Synthesis, biological evaluation, and molecular docking of Ugi products containing a zinc-chelating moiety as novel inhibitors of histone deacetylases. J Med Chem 52:2776–2785. doi:10.1021/jm801529c
14. Huang WJ, Chen CC, Chao SW, Lee SS, Hsu FL, Lu YL, Hung MF, Chang CI (2010) Synthesis of N-hydroxycinnamides capped with a naturally occurring moiety as inhibitors of histone deacetylase. Chem Med Chem 5:598–607. doi:10.1002/cmdc.200900494
15. Lu Q, Wang DS, Chen CS, Hu YD (2005) Structure-based optimization of phenylbutyrate-derived histone deacetylase inhibitors. J Med Chem 48:5530–5535. doi:10.1021/jm0503749
16. Mai A, Valente S, Nebbioso A, Simeoni S, Ragno R, Massa S, Brosch G, De Bellis F, Manzo F, Altucci L (2009) New pyrrole-based histone deacetylase inhibitors: binding mode, enzyme- and cell-based investigations. Int J Biochem Cell Biol 41:235–247. doi:10.1016/j.biocel.2008.09.002
17. Pirali T, Faccio V, Mossetti R, Grolla AA, Di Micco S, Bifulco G, Genazzani AA, Tron GC (2010) Synthesis, molecular docking and biological evaluation as HDAC inhibitors of cyclopeptide mimetics by a tandem three-component reaction and intramolecular [3+2] cycloaddition. Mol Divers 14:109–121. doi:10.1007/s11030-009-9153-9
18. Wang DF, Wiest O, Helquist P, Lan-Hargest HY, Wiech NL (2004) On the function of the 14 A long internal cavity of histone deacetylase-like protein: implications for the design of histone deacetylase inhibitors. J Med Chem 47:3409–3417. doi:10.1021/jm0498497
19. Ortore G, Di CF, Martinelli A (2009) Docking of hydroxamic acids into HDAC1 and HDAC8: a rationalization of activity trends and selectivities. J Chem Info Model 49:2774–2785. doi:10.1021/ci900288e
20. Wang DF, Helquist P, Wiech NL, Wiest O (2005) Toward selective histone deacetylase inhibitor design: homology modeling, docking studies, and molecular dynamics simulations of human class I histone deacetylases. J Med Chem 48:6936–6947. doi:10.1021/jm0505011
21. Estiu G, West N, Mazitschek R, Greenberg E, Bradner JE, Wiest O (2010) On the inhibition of histone deacetylase 8. Bioorg Med Chem 18:4103–4110. doi:10.1016/j.bmc.2010.03.080
22. Raha K, Merz KM Jr (2004) A quantum mechanics-based scoring function: study of zinc ion-mediated ligand binding. J Am Chem Soc 126:1020–1021. doi:10.1021/ja038496i
23. Irwin JJ, Raushel FM, Shoichet BK (2005) Virtual screening against metalloenzymes for inhibitors and substrates. Biochemistry 44:12316–12328. doi:10.1021/bi050801k
24. Park H, Lee S (2004) Homology modeling, force field design, and free energy simulation studies to optimize the activities of histone deacetylase inhibitors. J Comput Aided Mol Des 18:375–388. doi:10.1007/s10822-004-2283-3
25. Ryde U (1995) Molecular dynamics simulations of alcohol dehydrogenase with a four- or five-coordinate catalytic zinc ion. Proteins 21(1):40–56. doi:10.1002/prot.340210106
26. Somoza JR, Skene RJ, Katz BA, Mol C, Ho JD, Jennings AJ, Luong C, Arvai A, Buggy JJ, Chi E, Tang J, Sang BC, Verner E, Wynands R, Leahy EM, Dougan DR, Snell G, Navre M, Knuth MW, Swanson RV, McRee DE, Tari LW (2004) Structural snapshots of human HDAC8 provide insights into the class I histone deacetylases. Structure 12:1325–1334. doi:10.1016/j.str.2004.04.012

27. Sherman W, Day T, Jacobson MP, Friesner RA, Farid R (2006) Novel procedure for modeling ligand/receptor induced fit effects. J Med Chem 49:534–553. doi:10.1021/Jm050540c
28. Verdonk ML, Cole JC, Hartshorn MJ, Murray CW, Taylor RD (2003) Improved protein-ligand docking using GOLD. Proteins Struct Funct Gen 52:609–623. doi:10.1002/Prot.10465
29. Dowling DP, Gantt SL, Gattis SG, Fierke CA, Christianson DW (2008) Structural studies of human histone deacetylase 8 and its site-specific variants complexed with substrate and inhibitors. Biochemistry 47:13554–13563. doi:10.1021/bi801610c
30. Vannini A, Volpari C, Filocamo G, Casavola EC, Brunetti M, Renzoni D, Chakravarty P, Paolini C, De Francesco R, Gallinari P, Steinkuhler C, Di Marco S (2004) Crystal structure of a eukaryotic zinc-dependent histone deacetylase, human HDAC8, complexed with a hydroxamic acid inhibitor. Proc Natl Acad Sci USA 101:15064–15069. doi:10.1073/pnas.0404603101
31. Vannini A, Volpari C, Gallinari P, Jones P, Mattu M, Carfi A, De Francesco R, Steinkuhler C, Di Marco S (2007) Substrate binding to histone deacetylases as shown by the crystal structure of the HDAC8–substrate complex. EMBO Rep 8:879–884. doi:10.1038/sj.embor.7401047
32. He B, Velaparthi S, Pieffet G, Pennington C, Mahesh A, Holzle DL, Brunsteiner M, van Breemen R, Blond SY, Petukhov PA (2009) Binding ensemble profiling with photoaffinity labeling (BEProFL) approach: mapping the binding poses of HDAC8 inhibitors. J Med Chem 52:7003–7013. doi:10.1021/jm9005077
33. Neelarapu R, Holzle DL, Velaparthi S, Bai H, Brunsteiner M, Blond SY, Petukhov PA (2011) Design, synthesis, docking, and biological evaluation of novel diazide-containing isoxazole- and pyrazole-based histone deacetylase probes. J Med Chem 54:4350–4364. doi:10.1021/jm2001025
34. Bora-Tatar G, Dayangac-Erden D, Demir AS, Dalkara S, Yelekci K, Erdem-Yurter H (2009) Molecular modifications on carboxylic acid derivatives as potent histone deacetylase inhibitors: activity and docking studies. Bioorg Med Chem 17:5219–5228. doi:10.1016/j.bmc.2009.05.042
35. Kirchmair J, Markt P, Distinto S, Schuster D, Spitzer GM, Liedl KR, Langer T, Wolber G (2008) The protein data bank (PDB), its related services and software tools as key components for in silico guided drug discovery. J Med Chem 51:7021–7040. doi:10.1021/Jm8005977
36. Pettersen EF, Goddard TD, Huang CC, Couch GS, Greenblatt DM, Meng EC, Ferrin TE (2004) UCSF Chimera—a visualization system for exploratory research and analysis. J Comput Chem 25:1605–1612. doi:10.1002/jcc.20084
37. Eswar N, Webb B, Marti-Renom MA, Madhusudhan MS, Eramian D, Shen MY, Pieper U, Sali A (2007) Comparative protein structure modeling using MODELLER. Curr Protoc Prot Sci 2:2.9. doi:10.1002/0471140864.ps0209s50
38. Word JM, Lovell SC, Richardson JS, Richardson DC (1999) Asparagine and glutamine: using hydrogen atom contacts in the choice of side-chain amide orientation. J Mol Biol 285:1735–1747
39. Chemical Computing Group Inc. (2010) Molecular Operating Environment (MOE). Chemical Computing Group Inc., Montreal. http://www.chemcomp.com. 2010
40. Vanommeslaeghe K, Loverix S, Geerlings P, Tourwe D (2005) DFT-based ranking of zinc-binding groups in histone deacetylase inhibitors. Biorg Med Chem 13:6070–6082. doi:10.1016/j.bmc.2005.06.009
41. Jones G, Willett P, Glen RC (1995) Molecular recognition of receptor-sites using a genetic algorithm with a description of desolvation. J Mol Biol 245:43–53. doi:10.1016/S0022-2836(95)80037-9
42. Jain AN (2007) Surflex-Dock 2.1: robust performance from ligand energetic modeling, ring flexibility, and knowledge-based search. J Comput Aided Mol Des 21:281–306. doi:10.1007/s10822-007-9114-2
43. Mayo SL, Olafson BD, Goddard WA (1990) Dreiding—a generic force-field for molecular simulations. J Phys Chem 94:8897–8909. doi:10.1021/j100389a010
44. Pieffet G, Petukhov PA (2009) Parameterization of aromatic azido groups: application as photoaffinity probes in molecular dynamics studies. J Mol Model 15:1291–1297. doi:10.1007/s00894-009-0488-z
45. Jakalian A, Jack DB, Bayly CI (2002) Fast, efficient generation of high-quality atomic charges. AM1-BCC model: II. Parameterization and validation. J Comput Chem 23:1623–1641. doi:10.1002/Jcc.10128
46. Openeye Scientific Software (2010) molcharge. Openeye Scientific Software, Santa Fe
47. Guha R, Howard MT, Hutchison GR, Murray-Rust P, Rzepa H, Steinbeck C, Wegner J, Willighagen EL (2006) The Blue Obelisk—interoperability in chemical informatics. J Chem Info Model 46:991–998. doi:10.1021/ci050400b
48. R Foundation for Statistical Computing (2009) R: a language and environment for statistical computing. R Foundation for Statistical Computing, Vienna
49. Huang N, Shoichet BK (2008) Exploiting ordered waters in molecular docking. J Med Chem 51:4862–4865. doi:10.1021/jm8006239
50. Barril X, Fradera X (2006) Incorporating protein flexibility into docking and structure-based drug design. Expert Opin Drug Discov 1:1–14
51. Rueda M, Bottegoni G, Abagyan R (2010) Recipes for the selection of experimental protein conformations for virtual screening. J Chem Info Model 50:186–193. doi:10.1021/ci9003943
52. Yoon S, Welsh WJ (2004) Identification of a minimal subset of receptor conformations for improved multiple conformation docking and two-step scoring. J Chem Inf Comput Sci 44:88–96. doi:10.1021/ci0341619
53. Zhong H, Tran LM, Stang JL (2009) Induced-fit docking studies of the active and inactive states of protein tyrosine kinases. J Mol Graph Model 28:336–346. doi:10.1016/j.jmgm.2009.08.012
54. Barril X, Morley SD (2005) Unveiling the full potential of flexible receptor docking using multiple crystallographic structures. J Med Chem 48:4432–4443. doi:10.1021/Jm048972v
55. Wu R, Lu Z, Cao Z, Zhang Y (2011) Zinc chelation with hydroxamate in histone deacetylases modulated by water access to the linker binding channel. J Am Chem Soc 133:6110–6113. doi:10.1021/ja111104p
56. Wang D, Helquist P, Wiest O (2007) Zinc binding in HDAC inhibitors: a DFT study. J Org Chem 72:5446–5449. doi:10.1021/jo070739s
57. Gantt SL, Gattis SG, Fierke CA (2006) Catalytic activity and inhibition of human histone deacetylase 8 is dependent on the identity of the active site metal ion. Biochemistry 45:6170–6178. doi:10.1021/bi060212u
58. Chen Y, Lopez-Sanchez M, Savoy DN, Billadeau DD, Dow GS, Kozikowski AP (2008) A series of potent and selective, triazolylphenyl-based histone deacetylases inhibitors with activity against pancreatic cancer cells and *Plasmodium falciparum*. J Med Chem 51:3437–3448. doi:10.1021/jm701606b